



Published in final edited form as:

Invest Ophthalmol Vis Sci. 2008 July ; 49(7): 3107–3114.

Neutralizing VEGF Decreases Tortuosity and Alters Endothelial Cell Division Orientation in Arterioles and Veins in a Rat Model of ROP:

Relevance to Plus Disease

M. Elizabeth Hartnett^{1,2}, David Martiniuk¹, Grace Byfield¹, Pete Geisen¹, Gefei Zeng^{2,3}, and Victoria L. Bautch^{2,3}

¹Department of Ophthalmology, The University of North Carolina, Chapel Hill, North Carolina

²Carolina Cardiovascular Biology Center, The University of North Carolina, Chapel Hill, North Carolina

³Department of Biology, The University of North Carolina, Chapel Hill, North Carolina

Abstract

Purpose—To study the effects of vascular endothelial growth factor (VEGF) on endothelial nitric oxide synthetase (eNOS) and retinal vascular tortuosity and cleavage planes in a rat model of retinopathy of prematurity (ROP).

Methods—Within 4 hours of birth, pups and mothers were cycled between 50% and 10% oxygen daily. At postnatal day (p)12, pups received either intravitreal anti-rat neutralizing antibody to VEGF or control nonimmune rat IgG in one eye and returned to oxygen cycling until p14 when they were placed in room air (RA) for 4 days (50/10 oxygen-induced retinopathy [50/10 OIR]). Tortuosity indices and endothelial cleavage plane angles relative to the long axes of the major retinal vessels during anaphase were calculated from phosphohistone- and Alexa-isolectin-stained retinal flatmounts. Some retinas were processed for eNOS protein or phosphorylated/total eNOS.

Results—Retinas from 50/10 OIR had increased tortuosity over time with peaks at p12 and p14 ($P < 0.001$ vs. RA) before the development of intravitreal neovascularization, which peaked at p18. Compared with RA, eNOS/actin in 50/10 OIR retinas was increased at p12 ($P = 0.0003$) and p14 ($P = 0.047$). Inhibition of VEGF with a neutralizing antibody decreased tortuosity and caused endothelial mitosis cleavage planes to orient in favor of vessel elongation but did not affect eNOS protein or activation.

Conclusions—In the 50/10 OIR model, a model with relevance to ROP, arteriolar tortuosity, and venous dilation are increased through VEGF, which influences the orientation of endothelial cell cleavage in major arterioles and veins, independent of eNOS.

Plus disease, manifest by dilation and tortuosity of retinal vessels, is an important feature of severe retinopathy of prematurity (ROP) and is predictive of poor outcome and vision loss in preterm infants.¹ However, the causes of plus disease are incompletely understood. Better understanding of the mechanisms of plus disease may lead to earlier treatments or prevention of severe ROP.

Corresponding author: M. Elizabeth Hartnett, 6109A Neuroscience Research Building, Department of Ophthalmology, University of North Carolina, Chapel Hill, NC, 27599-7041; hartnet@med.unc.edu..

Disclosure: M.E. Hartnett, None; D. Martiniuk, None; G. Byfield, None; P. Geisen, None; G. Zeng, None; V.L. Bautch, None

The publication costs of this article were defrayed in part by page charge payment. This article must therefore be marked “advertisement” in accordance with 18 U.S.C. §1734 solely to indicate this fact.

Early investigators proposed that retinal vascular dilation and tortuosity in plus disease were a result of midperipheral mesenchymal shunting and increased retinal blood flow.² However, studies using color Doppler imaging to measure blood flow in the central retinal artery were in disagreement. In one study, there were no significant flow differences between preterm infants with and without ROP, and in infants with ROP, there were no flow differences between those with and without plus disease.³ In another study, there was reduced blood flow in infants with plus disease.⁴ Neither study showed increased blood flow as initially hypothesized. However, measurements of blood flow within the central retinal artery are difficult in infant eyes and may not reflect that in the mesenchymal shunt or peripheral vessels.

Increased blood flow increases shear stress, the in-plane frictional force, on endothelial cells within blood vessels. In tortuous vessels, the acutely curved part of the vessel is believed to have greater shear stress and the opposite side reduced shear stress. Shear stress can activate endothelial nitric oxide synthetase (eNOS) to produce nitric oxide (NO), which is important in vessel homeostasis.⁵⁻⁷ One outcome of NO is vascular muscle relaxation and vessel dilatation, which is a feature of plus disease in ROP.

Besides shear stress, other stimuli, including hypoxia and growth factors like vascular endothelial growth factor (VEGF) can increase eNOS expression.⁸ Hypoxia has been associated with arterial tortuosity after middle cerebral artery occlusion,⁹ and when hypoxia is chronic, tortuosity is believed to be a form of angiogenesis through vessel lengthening. VEGF is mechanistically involved in the intravitreal neovascularization that occurs in animal models of ROP,^{10,11} and VEGF RNA was increased in the retina in a human infant with ROP.¹² VEGF induces blood flow to ischemic myocardium by increasing collateral vessel formation,¹³ and VEGF also increases the size of capillaries during remodeling.¹⁴ VEGF is ineffective at improving angiogenesis in *enos*^{-/-} mice in a murine ischemic limb model, suggesting that eNOS may be a downstream mediator of VEGF.¹⁵ Finally, eNOS was shown to be involved in hyperoxia-induced vaso-oblivation and angiogenesis in an *enos*^{-/-} mouse model.¹⁶ In this last study, VEGF was not found to be downstream of eNOS. Therefore, eNOS can be activated by increased blood flow and hypoxia and may be a downstream mediator of VEGF-induced angiogenesis in some tissues.

We asked whether plus disease is in part related to increased VEGF bioactivity and, if so, whether eNOS is involved. We used the rat 50/10 oxygen-induced retinopathy (50/10 OIR) model, which develops peripheral avascular retina, intravitreal neovascularization, and arteriolar tortuosity similar to human ROP.^{17,18} We also measured the orientation of the cleavage of mitotic endothelial cells during anaphase¹⁹ within newly formed intraretinal arterioles and veins of pups in the 50/10 OIR model after treatment with a neutralizing antibody to VEGF as a method of assessing the effect of VEGF on dilation and tortuosity of large retinal vessels.

Materials and Methods

Animal Treatments

All animals were cared for in accordance with the Institute for Laboratory Animal Research (Guide for the Care and Use of Laboratory Animals) and the ARVO Statement for the Use of Animals in Ophthalmic and Vision Research.

Rat Model of Oxygen-Induced Retinopathy (50/10 OIR Model)

An oxygen cyclor (Oxycycler; Biospherix, New York, NY), which regulates the atmosphere inside an incubator by injecting either nitrogen or oxygen, was used to induce oxygen-induced retinopathy in newborn Sprague-Dawley rats (Charles River, Wilmington, MA). Within a few

hours of birth, pups designated postnatal age (p)0 and their mothers were placed in the incubator. Oxygen was cycled between 50% and 10% every 24 hours for 14 days, and then the pups were returned to room air (RA) for 4 additional days (50/10 OIR model).¹⁸ These oxygen extremes were similar to oxygen saturation measurements in a preterm infant in whom severe ROP develops.²⁰ In addition, in the rat, inspired oxygen has been directly related to blood oxygen level (Pao₂).²¹ Litters of 12 to 14 pups were used in all experiments. Carbon dioxide in the cage was monitored and flushed from the system by maintaining sufficient gas flow.

Neutralizing Antibody to VEGF as Intravitreal Injection

In each litter, half of the pups received an intravitreal injection of a rat neutralizing antibody against VEGF₁₆₄ (50 ng in 1 μ L; R&D Systems, Minneapolis, MN), in one eye and half of the litter received an intravitreal injection of 50 ng rat nonimmune IgG in one eye as the control. We chose the dose that we have reported to be effective in reducing intravitreal neovascularization in the 50/10 OIR model.¹¹ The fellow eyes were not injected. All intravitreal injections were performed with a 33-gauge needle inserted just behind the limbus, as previously described.¹¹ Injections were made at p12. Topical antibiotic ointment (0.5% erythromycin) was then applied to the eye, and the animals were returned to cycling for 2 days.

Dissecting Retinal Tissue for Flatmounting

The pups were heavily anesthetized by intraperitoneal (IP) injection of ketamine (2.5 mg/kg) and xylazine (1 mg/kg). Paraformaldehyde (PFA; 0.7-1.0 mL, 0.5%) was directly perfused into the left ventricle before euthanization by intracardiac injection of pentobarbital (80 mg/kg). Both eyes were enucleated, and whole eyes were fixed in 2% PFA for 2 hours. The retinas were carefully removed by using a modification of the method of Chan-Ling et al.²² Briefly, under a dissecting microscope an incision was made at the limbus, and the cornea was circumcised from the sclera. The lens was gently removed without disturbing the retina. The remaining eye cup was transferred to PBS, and the full extent of the retina with the ora serrata intact, was eased from the sclera using fine forceps. Care was taken to remove the hyaloidal vessels and any remaining vitreous. The retina was then placed onto a microscope slide and flattened by making four incisions, each 90° apart, beginning at the ora serrata and extending centrally from the equator stopping short of the optic nerve opening.

Flatmount Immunohistochemistry

The flattened retinas were made permeable in ice cold 70% vol/vol ethanol for 20 minutes, and then in PBS/1% Triton X-100 for 30 minutes. The retinas were incubated with Alexa Fluor 568 conjugated *Griffonia simplicifolia* (Bandeiraea) isolectin B4 (5 μ g/mL; Invitrogen-Molecular Probes, Eugene, OR) in PBS overnight at 4°C for staining of the vasculature. Some retinas were then placed in a blocking solution of PBS/1% Triton X-100 with 5% BSA for 1 hour before incubation overnight in rabbit polyclonal anti-phosphohistone H3 (10 μ g/mL; Upstate Biotechnology, Lake Placid, NY) at 4°C. The retinas were rinsed three times in PBS and then incubated in goat anti-rabbit Alexa Fluor 488-conjugated secondary antibody (1:100; Invitrogen-Molecular Probes) in PBS for 3 hours at 37°C. The retinas were rinsed three times in PBS and mounted in PBS:glycerol (2:1) with antifade medium (VectaShield; Vector Laboratories, Burlingame, CA), and the coverslip was sealed with nail polish. Images of retinal vasculature were captured with an inverted microscope (TE2000U; Nikon, Tokyo, Japan) and an inverted fluorescence-differential interference contrast (DIC) microscope (Leica Microsystems, Bannockburn, IL) (microscopy performed at the Michael-Hooker Microscopy Facility, University of North Carolina at Chapel Hill) and digitally stored for analysis. Image sections were stitched on computer (PhotoFit Premium 1.44; Tekmate, Anchor-age, AK).

Quantitative Analysis of Cell Division Orientation

Quantitative image analysis was performed using the freeware Image-Tool, version 3 (University of Texas, Austin, TX). Cell division cleavage planes were identified in Alexa Fluor 568-conjugated isolectin-stained vessels by bisection of the separating chromosomes labeled with Alexa Fluor 488-conjugated anti-phosphohistone H3 during late metaphase to anaphase. Lines were drawn with image management software (Photoshop 7.0; Adobe, San Jose, CA) along the cleavage plane and along the long axis of the blood vessel for each mitotic division, and the angle between these two lines was calculated. Angles of 0° to 10° are divisions whose cleavage planes are near parallel to the long axis of the blood vessel, whereas angles of 80° to 90° are divisions whose cleavage planes are perpendicular to the long axis of the blood vessel. Angles were then grouped to every 10°, ranging from 0° to 90°. ¹⁹

Determination of Arteriole and Vein Tortuosity

The tortuosity indices of major retinal arterioles and veins were determined by ROPtool, version 1.1, from the University of North Carolina Computer-Aided Diagnosis and Display Laboratory. ²³ The software automatically traces the course of major posterior pole vessels and expresses the tortuosity index as a ratio of the actual length of the vessel in pixels over the straight distance from end to end.

Fresh Tissue Preparation

The animals were euthanized with an overdose of pentobarbital (80 mg/kg IP). Both eyes were enucleated, and the retinas were isolated under a dissecting microscope in similar fashion as for flat mounting, except that the ora serrata was carefully removed. The tissue was placed in radioimmunoprecipitation assay (RIPA) buffer (20 mM Tris Base, 120 mM NaCl, 1% Triton x-100, 0.5% sodium deoxycholate, 0.1% SDS, 10% glycerol) with protease inhibitor cocktail and sodium orthovanadate (both 1:100; Sigma-Aldrich, St. Louis, MO) for Western blot analysis, or mammalian protein extraction reagent (M-Per) for ELISA and frozen at -20°C until analysis.

Protein Extraction, Immunoprecipitation, and Western Blot Analysis

Freshly dissected unfixed retinal tissue immersed in RIPA buffer was placed on ice for 10 minutes. The tissue was homogenized, and lysates were centrifuged at maximum speed for 10 minutes at 4°C. The supernatants were collected, and total protein in the cell lysate was determined by the BCA (bicinchoninic acid) protein assay (Pierce Biotechnology, Rockford, IL). For phosphorylated eNOS, 50 µg of each protein sample was incubated with 1 µg eNOS (NOS3) antibody (sc-654; Santa Cruz Biotechnology, Santa Cruz, CA) at 4°C overnight. The immune complexes were captured by incubation with protein G sepharose beads (GE Healthcare, Stockholm, Sweden) at 4°C for 1 hour, and the collected beads were washed three times in RIPA buffer and centrifuged at 3000g for 2 minutes at 4°C between washes. The bound protein-bead complexes were eluted with sample buffer, boiled for 10 minutes, and separated by sodium dodecyl sulfate-poly-acrylamide gel electrophoresis (SDS-PAGE). After transfer to polyvinylidene fluoride (PVDF) membrane (Millipore, Billerica, MA), according to standard protocols, the blots were blocked in 5% BSA/TBST for 1 hour at room temperature, then incubated in phospho-serine antibody (1:1000, AB1603; Chemicon, Temecula, CA) overnight with gentle agitation at 4°C. Membranes were then stripped with Western blot stripping buffer (Restore Plus; 46430; Pierce Biotechnology) according to the manufacturer's protocol and reprobbed with eNOS antibody (1:1000; Santa Cruz Biotechnology). For total eNOS or β-actin analysis, 50 µg of total protein from cell lysate supernatants were diluted in sample buffer, boiled, and run for SDS-PAGE as just described. The blocked membranes were incubated with gentle agitation in either eNOS antibody (1:1000; Santa Cruz Biotechnology) overnight at 4°C or β-actin-HRP antibody (1:20000; AbCam, Cambridge, MA) for 1 hour at

room temperature. After four washes, the blots were incubated 1 hour with horseradish peroxidase (HRP)-conjugated secondary antibody and washed with Tris-buffered saline with Tween-20 (TBST). Visualization was performed using the enhanced chemiluminescence (Pierce Biotechnology). The signal intensity was quantified using analysis software (UN-SCAN-IT ver.6.1; Silk Scientific, Orem, UT). Rat aorta was used as a positive control.

Statistical Analysis

For Western blot experiments based on time point of analysis, the data were analyzed by Student's *t*-test. In cases in which more than two treatment groups were analyzed, an overall analysis of variance (ANOVA) was performed with post hoc protected Bonferroni *t*-tests (SPSS ver. 14; SPSS, Chicago, IL). In analyses in which the distribution of outcomes within treatment and control groups was tested, the χ^2 test was used. For all comparisons, an α level of <0.05 was used as the criterion of significance.

Results

Increased Arteriolar Tortuosity in the 50/10 OIR Model

Compared with RA control animals, retinal arterioles in rats in the 50/10 OIR model showed a tendency toward increased tortuosity indices after p6. There was some variability in the tortuosity index based on whether pups had just been exposed to hypoxia (even postnatal days followed the 0% O₂ cycle) or hyperoxia (odd postnatal days followed the 50% O₂ cycle), with a trend toward greater tortuosity after hypoxia. Compared with RA control animals, the tortuosity index was significantly greater in eyes in the 50/10 OIR model at p12 after hypoxia, and at p14 after 2 days in RA (Fig. 1 ANOVA, $P < 0.001$, post hoc protected *t*-test $P < 0.001$). In addition, the tortuosity indices at p12 and p14 were significantly greater than those in the 50/10 OIR at p7, p11, and p18. There was no difference in venous tortuosity index in the 50/10 OIR compared with RA control eyes or over time in the 50/10 OIR model (data not shown).

Increased Tortuosity Associated with Increased eNOS but Not Activated eNOS in 50/10 OIR

We and others previously found that retinal VEGF protein was increased in the 50/10 OIR model compared with RA controls at p12, p14, and at p18, the time of maximum intravitreal neovascularization, and that the peak concentration of VEGF occurred at p14.^{10,11} Because VEGF or blood flow induce shear stress, or both can increase eNOS expression and activation in other tissues,⁵⁻⁷ we measured eNOS and phosphorylation of eNOS at p12 and p14, time points when the tortuosity index was also significantly greater in the 50/10 OIR model compared with RA (Fig. 1). We found that eNOS/actin was increased at p12 ($P = 0.0003$, *t*-test) and p14 ($P = 0.047$), compared with RA (*t*-test; Fig. 2). We found no difference in eNOS/actin at p18 when the tortuosity index was reduced and did not find activation of eNOS determined by measuring phosphorylated eNOS/total eNOS at p12 (data not shown).

VEGF Causes Tortuosity in the 50/10 OIR Model

To study the possible effects of VEGF on the development of tortuosity, we compared eyes treated with a 50-ng dose of a neutralizing antibody to VEGF, which we had found to be effective in inhibiting intravitreal neovascularization in the 50/10 OIR model, with IgG-treated control eyes.¹¹ The tortuosity index was significantly decreased at p14 in retinal vessels after a single dose of 50 ng neutralizing VEGF antibody given at p12 (Fig. 3), but the effect was not present at p18 (data not shown). In part, this may have been because retinal tortuosity became less in the 50/10 OIR model by p18 (Fig. 1).

Effect of Neutralizing VEGF with Antibody on eNOS

Investigators have reported eNOS to be a downstream mediator of VEGF-induced angiogenesis in other tissues.¹⁵ Since increased eNOS protein was associated with the time points of greatest tortuosity and neutralizing the bioactivity of VEGF with an antibody to VEGF₁₆₄ reduced tortuosity in the 50/10 OIR model, we wanted to determine whether inhibiting VEGF with a neutralizing antibody would reduce eNOS. We found that 50 ng of a neutralizing antibody to VEGF did not change eNOS concentration relative to actin (Fig. 4) or phosphorylated/total eNOS at p14 (Fig. 5).

Effect of VEGF on Orientation of Endothelial Cell Cleavage Planes

We have shown in a prior study that increased signaling through VEGF receptor 2 (VEGFR2) in an *flt-1*^{-/-} embryonic stem cell model, a model lacking blood flow, results in more randomly oriented endothelial cell cleavage planes, measured during the anaphase, compared with the control, and this pattern is rescued with a soluble *flt-1* transgene linked to the PECAM promoter/enhancer.¹⁹ We have also shown that inhibition of the bioactivity of VEGF with a neutralizing antibody reduces intraretinal signaling through VEGFR2 in the 50/10 OIR model, particularly in the inner vascular plexus.¹¹ We wanted to determine whether endothelial cleavage plane orientation was altered in the large vessels in the 50/10 OIR model, favoring dilation and tortuosity such as that in human plus disease and whether reducing VEGFR2 signaling with a neutralizing antibody to VEGF would restore the orientation of endothelial cell divisions such as that in normal development in RA. The angle between the cleavage plane of phosphohistone-stained mitotic figures determined during the anaphase and vessel long axis was determined in major vessels within the retinas of RA-raised and in VEGF antibody-treated, control IgG-treated, and noninjected eyes (Figs. 6E, 6F).

In RA-raised rats, the total number of mitoses identified per retina decreased with increasing postnatal age (38.83 at p6, 0 at p14; Table 1), with veins having more mitoses than arterioles. When only analyzing mitotic figures in the anaphase, there were few cleavage planes in both arterioles and veins in RA-raised rats. The prevalence of cleavage planes at 80° to 90° from the vessel long axis (favoring vessel elongation) increased with age of development in both arterioles and veins (Figs. 6A, 6B).

From two litters of rats raised in the 50/10 OIR model, pups received an intravitreal injection of either 50 ng neutralizing antibody to VEGF or IgG in one eye at p12 and were analyzed at p14. There were more mitotic events in the 50/10 OIR model than RA at p14 (Table 1). Within the 50/10 OIR model, there were slightly fewer mitoses, although not significantly so, in eyes that had received the neutralizing antibody to VEGF compared to IgG (Table 1).

We found that arterioles of pups treated with intravitreal injections of neutralizing antibody to VEGF₁₆₄ appeared to have a greater number of cleavage planes in anaphase that were between 80° and 90°, relative to the long axis of the vessel compared with control IgG treated eyes (Fig. 6C). This orientation, which causes elongation of the retinal vessel, corresponded more closely to that in normal development in RA-raised pups, in which fewer cleavage planes were found, but most occurred at the axis 70° to 90° from the long axis of the developing vessel¹⁹ (Fig. 6A). Furthermore, veins treated with VEGF antibody had fewer cleavage planes that were between 0° and 20° relative to the long axis of the vessel, compared with veins in IgG-injected control eyes ($P < 0.05$, χ^2 ; Fig. 6D). This result suggests that treatment with antibody to VEGF reduces venous dilation, a feature present in human plus disease.

Discussion

We found, in agreement with other investigators, that arteriolar tortuosity was increased in the rat 50/10 OIR model of ROP compared with RA-raised rats.¹⁷ We had previously measured retinal VEGF protein in the 50/10 OIR model and found significantly greater protein at p12, p14, and p18 compared with RA, with the peak concentration of retinal VEGF occurring at p14.^{10,11} The p12 and p14 time points also correspond to the time points with significantly higher tortuosity indices in the 50/10 OIR model compared with the RA control. Furthermore, retinal eNOS was increased at p12 and p14 compared with the RA control at the same time points that tortuosity and VEGF were increased, and these time points preceded the development of intravitreal neovascularization.^{10,11} However, although eNOS has been shown to be downstream of VEGF signaling in other tissues,⁸ we were unable to provide evidence that inhibition of VEGF with a neutralizing antibody, effective at reducing tortuosity and intravitreal neovascularization in the 50/10 OIR model,¹¹ had an effect on eNOS concentration or activation. We interpret these data to mean that the effects of VEGF on tortuosity are independent or downstream of eNOS. Brooks et al.¹⁶ found that in *enos*^{-/-} mice, hyperoxia-induced vaso-obliteration was less severe, but that VEGF concentration was not affected and did not appear to be downstream of eNOS signaling. Beauchamp et al.²⁴ found, also using the mouse OIR model, that NO had opposing effects on vaso-obliteration and VEGFR2 expression that depended on the redox state of the retina. Both these studies used constant high oxygen exposure in the mouse OIR model, which differs from the fluctuations and oxygen extremes used in the rat 50/10 OIR model. Based on our data and that in the literature, we speculate that the increase in eNOS seen by Western blot at p12 and p14 in the 50/10 OIR model may be related to other effects,^{24,25} including hypoxia and increased shear stress,⁸ and not directly to VEGF. Although previous studies, failed to show increased blood flow in human ROP by Doppler imaging,^{3,4} the techniques are difficult in infants. Furthermore, blood flow-induced shear stress in a tortuous vessel is complex. Whereas, in a straight vessel, shear stress is increased throughout the inner circumference of the vessel when blood flow increases,²⁶ in tortuous vessels and at branch points, the relationships within vessels and the signaling within endothelial cells are changed.²⁶ Blood flow measurements and shear stress may vary at different regions within the tortuous vessel. Therefore, it is conceivable that increased shear stress may occur in tortuous vessels and activate eNOS without registering an increase in blood flow measurements.

We inhibited VEGF with a neutralizing antibody at a concentration that we had found to reduce intravitreal neovascularization and intraretinal VEGFR2 signaling.¹¹ We found that arteriolar tortuosity was reduced, and the orientation of endothelial cell cleavage planes during the anaphase of the major veins and arterioles within the vascularized retina was changed. In veins, treatment with VEGF antibody caused a change from a parallel orientation of cleavage planes to the vessel long axis favoring vessel widening to one in which cleavage planes were perpendicular to the vessel long axis favoring vessel elongation. In arterioles, treatment with VEGF antibody caused a change from random cleavage plane orientation to one favoring vessel elongation similar to that found in RA in normal development¹⁹ and in agreement with our findings of reduced tortuosity in eyes treated with VEGF antibody. We had reported that increased signaling through VEGFR2 alters the organized orientation of endothelial cell cleavage planes determined during anaphase in an embryonic stem cell model in *flt-1*^{-/-} mice.¹⁹ In development, *flt-1* (murine name for VEGFR1) acts as a trap for VEGF, thus regulating the amount of VEGF present to signal through VEGFR2,²⁷ the receptor deemed to be more involved in the angiogenic processes.²⁸ Genetic deletion of *flt-1* is lethal in vivo, but it can be studied in the embryonic stem cell model and provides a means to induce a gain in VEGF signaling through VEGFR2. The data from the embryonic stem cell model demonstrated that the orientation of daughter cell divisions is necessary in blood vessel morphogenesis and is regulated by signaling through VEGFR2 in a flow-independent manner.¹⁹ These findings

contrasted with previous ones that proposed that shear stress is necessary and plays a major role in the morphogenesis of blood vessels.²⁹ Thus, it appears that shear stress is not necessary for regulating the orientation of daughter cell cleavage planes in developing tissue. In our present study, we found that VEGF was important in the orientation of cleavage planes of endothelial cells, this time in recently developed major vessels in retinas with blood flow. However, it appeared that although eNOS, activated by shear stress,⁵⁻⁷ was increased in the 50/10 OIR model, it was not involved in VEGF induced tortuosity and dilation. Although remodeling of capillaries during development in the rat eye has been carefully described,³⁰ our findings suggest that already-developed major intraretinal vessels, not just the newly formed capillaries, have endothelial divisions that are influenced by VEGF concentration. The importance of VEGF in human retinal and iris vessel dilatation and engorgement has been reported in a case series of human infants with aggressive posterior ROP, who experienced reduction in vessel tortuosity and dilation after treatment with bevacizumab, a monoclonal antibody against VEGF.³¹

VEGF is known to affect vascular development by influencing several events, including the number of endothelial tip cells to stalk cells,³² the direction in which filopodia point,³³ and endothelial cell proliferation and migration.³⁴ Once vessels have formed, how VEGF alters vessel diameter or tortuosity is largely unknown. However, based on development in other tissues, we know the orientation of the cleavage plane in dividing cells is regulated, in part, by the actin cytoskeleton.²⁹ Although the major vessels in the retina have already developed, our data show that mitoses are ongoing at least through p14 in the 50/10 OIR model. VEGF has been shown to induce actin cytoskeletal changes through signaling through integrins³⁵ or through activation of Rho GTPases,³⁶ for example, and through such cytoskeletal events, it is possible that the orientation of the cleavage planes during anaphase are altered.

In summary, our findings provide support that the causes of vascular tortuosity and dilation in the 50/10 OIR model, relevant to human ROP, are from increased VEGF signaling through VEGFR2,¹⁹ based on previous studies in which the same model, means of inhibition of VEGF, and dose were used.¹¹ Our data support that VEGF is an early event in the development of tortuosity and dilation. Although eNOS expression is increased in the 50/10 OIR model, our data do not support eNOS as downstream of VEGF-induced tortuosity and dilation in the 50/10 OIR model of ROP.

Acknowledgments

The authors thank David Sutton, MD (Department of Ophthalmology, University of North Carolina), Zheen Zhao, PhD (Department of Radiology, Duke University), Stephen Aylward, PhD (Kitware, Inc.), and David Wallace, MD (Department of Ophthalmology, Duke University) for assistance with image analysis.

Supported by National Eye Institute Grants R01 EY015130 (MEH) and R01 HL86564 (VLB) and Research to Prevent Blindness (MEH).

References

1. The Early Treatment for Retinopathy of Prematurity Cooperative Group. The Early Treatment for Retinopathy of Prematurity Study: structural findings at age 2 years. *Br J Ophthalmol* 2006;90:1378–1382. [PubMed: 16914473]
2. Kushner BJ, Essner D, Cohen JJ, Flynn JT. Retrolental fibroplasia. II. Pathologic correlation. *Arch Ophthalmol* 1977;95:29–38. [PubMed: 576397]
3. Holland D, Saunders R, Kagemann L, et al. Color Doppler imaging of the central retinal artery in premature infants undergoing examination for retinopathy of prematurity. *J AAPOS* 1999;3:194–198. [PubMed: 10477220]
4. Niwald A, Gralek M. Evaluation of blood flow in the ophthalmic artery and central retinal artery in children with retinopathy of prematurity. *Klinika Oczna* 2006;108:32–35. [PubMed: 16883936]

5. Cheng C, van Haperen R, de Waard M, et al. Shear stress affects the intracellular distribution of eNOS: direct demonstration by a novel in vivo technique. *Blood* 2005;106:3691–3698. [PubMed: 16105973]
6. Li H, Wallerath T, Forstermann U. Physiological mechanisms regulating the expression of endothelial-type NO synthase. *Nitric Oxide* 2002;7:132–147. [PubMed: 12223183]
7. Porth, C., editor. *Essentials of Pathophysiology: Concepts of Altered Health States*. 2nd ed.. Wolters Kluwer; Philadelphia: 2006. p. 342
8. Tai SC, Robb GB, Marsden PA. Endothelial nitric oxide synthase: a new paradigm for gene regulation in the injured blood vessel. *Arterioscler Thromb Vasc Biol* 2004;24:405–412. [PubMed: 14656742]
9. Coyle P. Diameter and length changes in cerebral collaterals after middle cerebral artery occlusion in the young rat. *Anat Record* 1984;210:357–364. [PubMed: 6507901]
10. Werdich XQ, Penn JS. Specific involvement of Src family kinase activation in the pathogenesis of retinal neovascularization. *Invest Ophthalmol Vis Sci* 2006;47:5047–5056. [PubMed: 17065526]
11. Geisen P, Peterson L, Martiniuk D, et al. Neutralizing antibody to VEGF reduces intravitreal neovascularization and does not interfere with vascularization of avascular retina in an ROP model. *Mol Vis* 2008;11:345–357. [PubMed: 18334951]
12. Young TL, Anthony DC, Pierce E, Foley E, Smith LEH. Histopathology and vascular endothelial growth factor in untreated and diode laser-treated retinopathy of prematurity. *J AAPOS* 1997;1:105–110. [PubMed: 10875087]
13. Banai S, Jaklitsch MT, Shou M, et al. Angiogenic-induced enhancement of collateral blood flow to ischemic myocardium by vascular endothelial growth factor in dogs. *Circulation* 1994;89:2183–2189. [PubMed: 7514110]
14. Rissanen TT, Korpisalo P, Markkanen JE, et al. Blood flow remodels growing vasculature during vascular endothelial growth factor gene therapy and determines between capillary arterialization and sprouting angiogenesis. *Circulation* 2005;112:3937–3946. [PubMed: 16344386]
15. Murohara T, Asahara T, Silver M, et al. Nitric oxide synthase modulates angiogenesis in response to tissue ischemia. *J Clin Invest* 1998;101:2567–2578. [PubMed: 9616228]
16. Brooks SE, Gu X, Samuel S, et al. Reduced severity of oxygen-induced retinopathy in eNOS-deficient mice. *Invest Ophthalmol Vis Sci* 2001;42:222–228. [PubMed: 11133872]
17. Liu K, Akula JD, Falk C, Hansen RM, Fulton AB. The retinal vasculature and function of the neural retina in a rat model of retinopathy of prematurity. *Invest Ophthalmol Vis Sci* 2006;47:2639–2647. [PubMed: 16723481]
18. Penn JS, Henry MM, Tolman BL. Exposure to alternating hypoxia and hyperoxia causes severe proliferative retinopathy in the newborn rat. *Pediatr Res* 1994;36:724–731. [PubMed: 7898981]
19. Zeng G, Taylor SM, McColm JR, et al. Orientation of endothelial cell division is regulated by VEGF signaling during blood vessel formation. *Blood* 2007;109:1345–1352. [PubMed: 17068148]
20. Cunningham S, Fleck BW, Elton RA, McIntosh N. Transcutaneous oxygen levels in retinopathy of prematurity. *Lancet* 1995;346:1464–1465. [PubMed: 7490994]
21. Penn JS, Henry MM, Wall PT, Tolman BL. The range of PaO₂ variation determines the severity of oxygen induced retinopathy in newborn rats. *Invest Ophthalmol Vis Sci* 1995;36:2063–2070. [PubMed: 7657545]
22. Chan-Ling T. Glial, vascular and neuronal cytotogenesis in whole-mounted cat retina. *Microsc Res Tech* 1997;36:1–16. [PubMed: 9031257]
23. Aylward SR, Bullitt E. Initialization, noise, singularities, and scale in height ridge traversal for tubular object centerline extraction. *IEEE Trans Med Imaging* 2002;21:61–75. [PubMed: 11929106]
24. Beauchamp MH, Sennlaub F, Speranza G, et al. Redox-dependent effects of nitric oxide on microvascular integrity in oxygen-induced retinopathy. *Free Radic Biol Med* 2004;37:1885–1894. [PubMed: 15528047]
25. Loufrani L, Retailleau K, Bocquet A, et al. Key role of the $\alpha 1$ - $\beta 1$ integrin in the activation of PI3Kinase-Akt by flow (shear stress) in resistance arteries. *Am J Physiol Heart Circ Physiol* 2008;294(4):H1906–H1913. [PubMed: 18245559]
26. Chien S. Effects of disturbed flow on endothelial cells. *Ann Biomed Eng* 2008;36(4):554–562. [PubMed: 18172767]

27. Hiratsuka S, Minowa O, Kuno J, Noda T, Shibuya M. Flt-1 lacking the tyrosine kinase domain is sufficient for normal development and angiogenesis in mice. *Proc Natl Acad Sci USA* 1998;95:9349–9354. [PubMed: 9689083]
28. Rahimi N. Vascular endothelial growth factor receptors: molecular mechanisms of activation and therapeutic potentials. *Exp Eye Res* 2006;83:1005–1016. [PubMed: 16713597]
29. Noria S, Xu F, McCue S, et al. Assembly and reorientation of stress fibers drives morphological changes to endothelial cells exposed to shear stress. *Am J Pathol* 2004;164:1211–1223. [PubMed: 15039210]
30. Ishida S, Yamashiro K, Usui T, et al. Leukocytes mediate retinal vascular remodeling during development and vaso-obliteration in disease. *Nat Med* 2003;9:781–789. [PubMed: 12730690]
31. Travassos A, Teixeira S, Ferreira P, et al. Intravitreal bevacizumab in aggressive posterior retinopathy of prematurity. *Ophthalmic Surg Lasers Imaging* 2007;38:233–237. [PubMed: 17552391]
32. Hellstrom M, Phng LK, Hofmann JJ, et al. Dll4 signalling through Notch1 regulates formation of tip cells during angiogenesis. *Nature* 2007;445:776–780. [PubMed: 17259973]
33. Gerhardt H, Golding M, Fruttiger M, et al. VEGF guides angiogenic sprouting utilizing endothelial tip cell filopodia. *J Cell Biol* 2003;161:1163–1177. [PubMed: 12810700]
34. Chan-Ling T, Gock B, Stone J. The effect of oxygen on vasoformative cell division: Evidence that ‘physiological hypoxia’ is the stimulus for normal retinal vasculogenesis. *Invest Ophthalmol Vis Sci* 1995;36:1201–1214. [PubMed: 7775098]
35. Mahabeleshwar GH, Feng W, Reddy K, Plow EF, Byzova TV. Mechanisms of integrin vascular endothelial growth factor receptor cross-activation in angiogenesis. *Circ Res* 2007;101:570–580. [PubMed: 17641225]
36. Sun H, Breslin JW, Zhu J, Yuan SY, Wu MH. Rho and ROCK signaling in VEGF-induced microvascular endothelial hyperpermeability. *Microcirculation* 2006;13:237–247. [PubMed: 16627366]

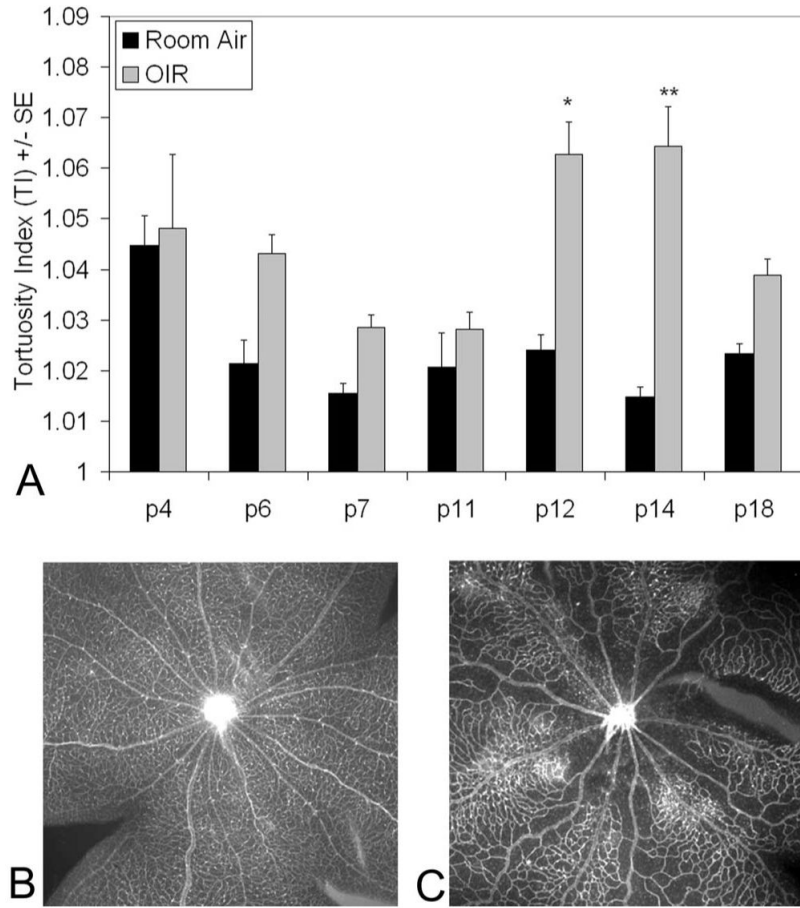


Figure 1. Arteriole tortuosity index of retinas at given postnatal days in RA or 50/10 OIR model (OIR). (A) Tortuosity was significantly greater in OIR retinas compared to RA (overall ANOVA $P < 0.0001$) at time points p12 ($*P < 0.0001$, post hoc protected Bonferroni t -test) and p14 ($**P < 0.001$, post hoc protected Bonferroni t -test). Tortuosity was also significantly increased in p12 ($P < 0.01$, Bonferroni post hoc corrected t -test) and p14 retinas ($P < 0.005$, Bonferroni t -test) compared with p7, p11, or p18 OIR. A minimum of four retinas was analyzed for each group. (B) Examples of retinas from p14 RA eyes and (C) p14 OIR eyes resulted in tortuosity indices of 1.021 ± 0.004 and 1.052 ± 0.013 , respectively.

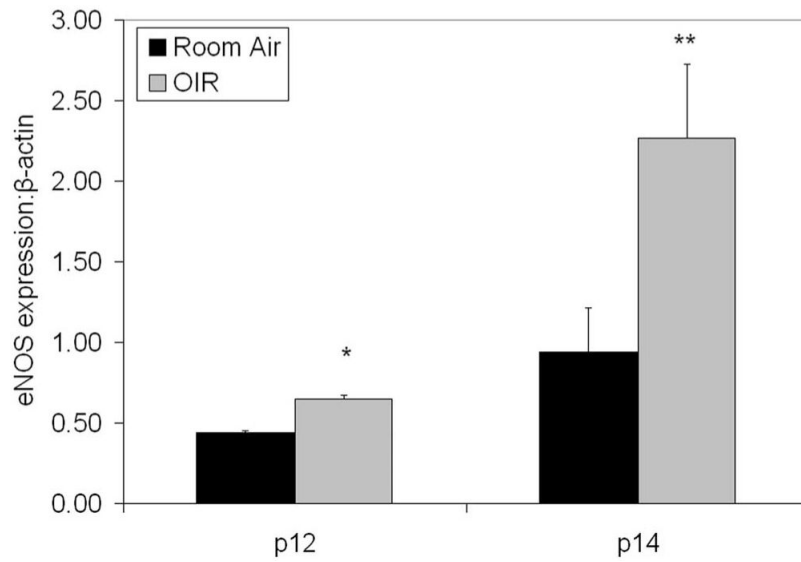


Figure 2. eNOS protein expression in retinas at p12 or p14 in RA or 50/10 OIR model (OIR) determined by Western blot. eNOS concentration (as a ratio to β -actin) in OIR and RA retinas at p12 (* $P = 0.0003$, t -test) and p14 (** $P = 0.047$, t -test). A minimum of four retinas was analyzed for each group.

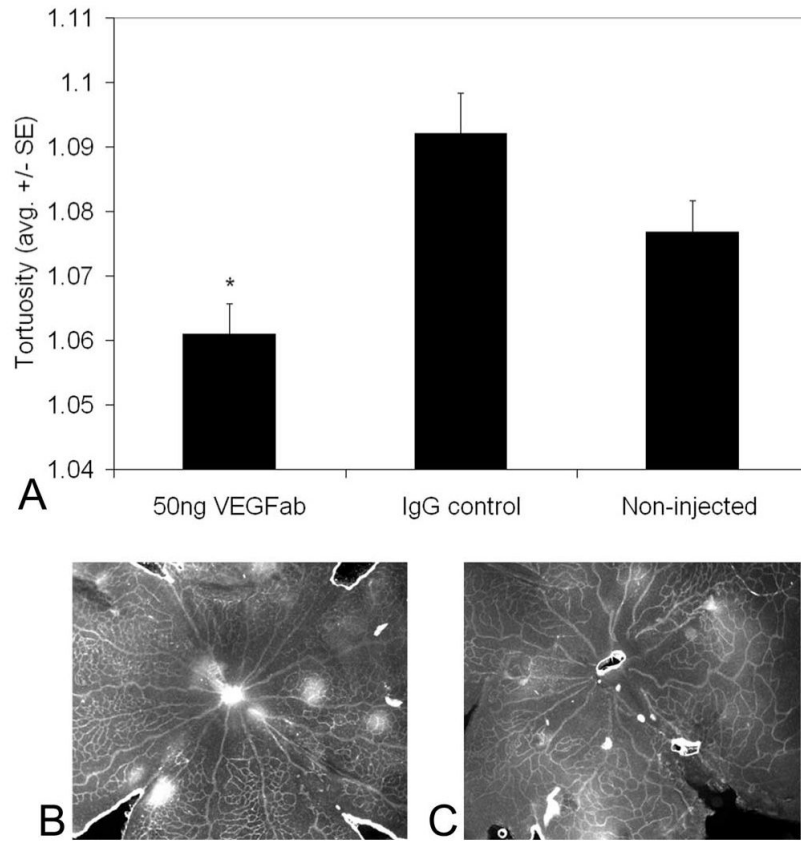


Figure 3. Arteriolar tortuosity index of retinas from eyes injected with either 50 ng VEGF antibody (VEGFab) or 50 ng control IgG at p12 and analyzed at p14. **(A)** The tortuosity index was significantly reduced in eyes injected with 50 ng VEGFab compared with that in IgG-injected eyes (ANOVA $*P = 0.004$, post hoc protected *t*-test). A minimum of four retinas was analyzed for each group. **(B)** Examples of retinas from eyes injected with 50 ng VEGFab and **(C)** 50 ng control IgG resulted in tortuosity indices of 1.03 ± 0.007 and 1.11 ± 0.04 , respectively.

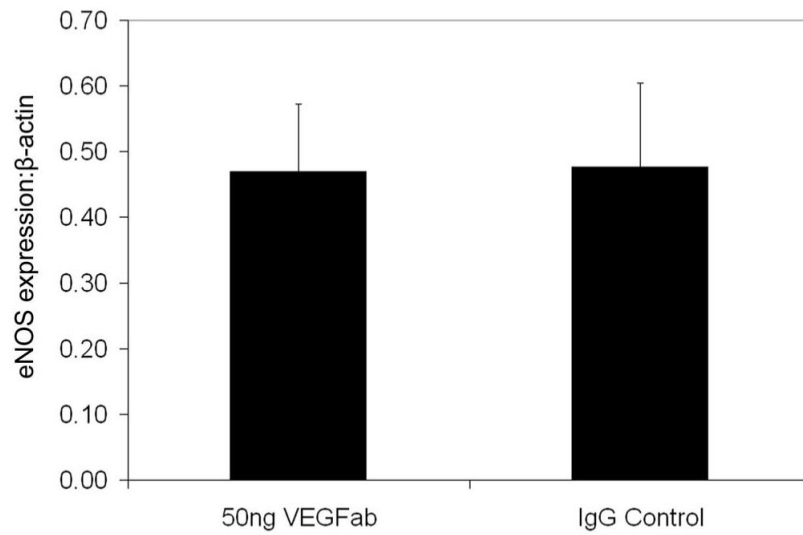


Figure 4. eNOS to β -actin protein expression determined by Western blot in whole retinas from 50/10 OIR rat pup eyes treated with either 50 ng neutralizing antibody to VEGF (VEGFab) or rat nonimmune IgG (IgG) at p12 and assayed at p14. Ten retinas were analyzed for each group.

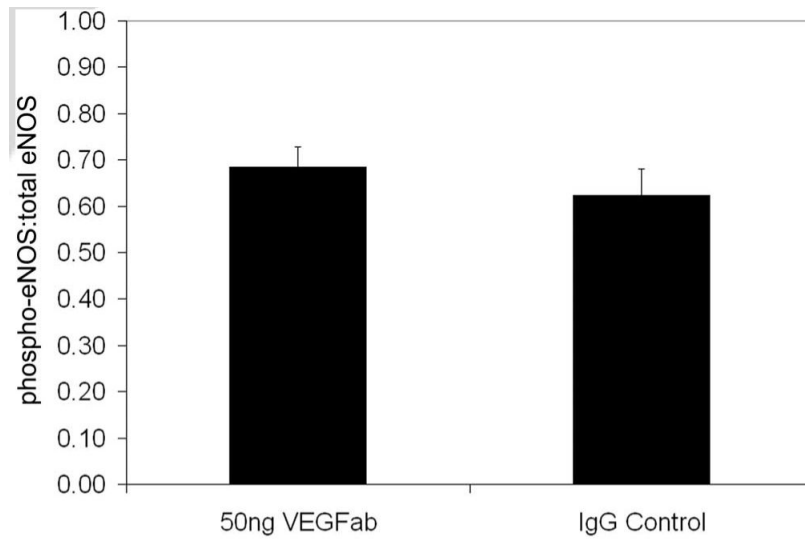
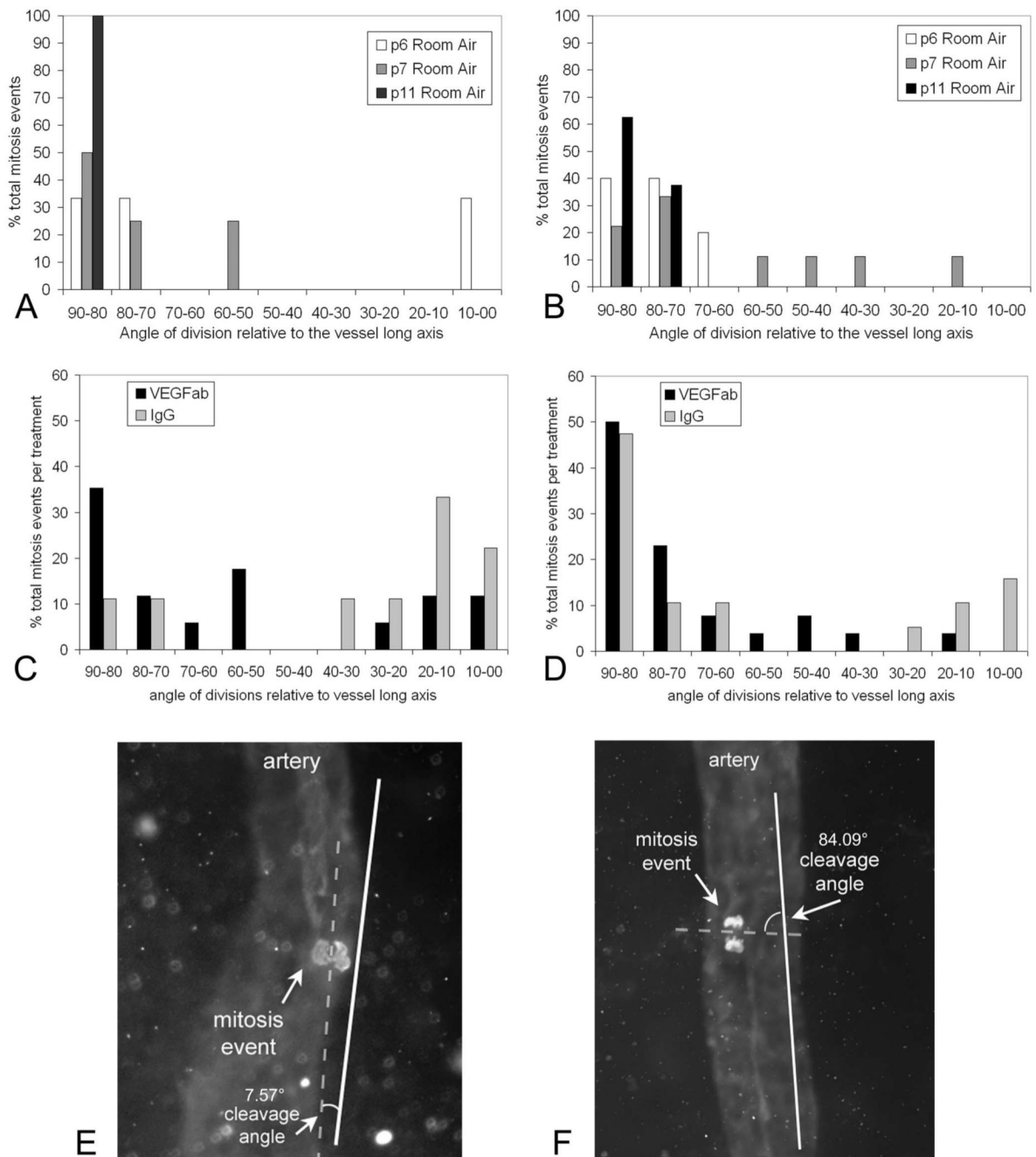


Figure 5. Phosphorylated eNOS to total eNOS protein determined by immunoprecipitation and Western blot in whole retinas from 50/10 OIR rat pup eyes treated with either 50 ng neutralizing antibody to VEGF (VEGFab) or rat nonimmune IgG (IgG) at p12 and assayed at p14. A minimum of nine retinas was analyzed for each group.

**Figure 6.**

(A) Arteriolar and (B) venous cleavage planes in normal retinal vascular development at p5, p6, and p11. By p14 and p15 when development of the inner retinal vascular plexus is complete, no mitosis planes were found in each of five retinas surveyed. (C) Angle of arteriole and (D) venous retinal endothelial cell division planes, grouped by degrees from the long axis of the vessel, in 50/10 OIR pups injected with either 50 ng VEGF or 50 ng control IgG. A value of 90° is perpendicular to the vessel long axis, and 0° is parallel to the vessel long axis.

Treatment with neutralizing antibody to VEGF caused veins to have fewer cleavage planes that were between 0° and 20° relative to the long axis of the vessel compared to IgG injected controls ($P < 0.05$, χ^2). These data provide support that treatment with antibody to VEGF

reduces venous dilation. **(E)** Retinal flatmount from rat pup in 50/10 OIR treated with 50 ng intravitreal VEGFab and colabeled with isolectin for retinal vessels and phosphohistone to stain mitoses. Angle between mitotic cleavage plane of dividing endothelial cell and long axis of the vessel measures 7.57° . **(F)** Flatmount of retina from an eye injected with 50 ng VEGFab showing a mitotic cleavage angle of 84.09° .

Number of Total Mitoses and Endothelial Cleavage Planes (during the Anaphase) in Arterioles and Veins in RA and 50/10 OIR

Table 1

Condition	Arterioles		Veins		All Major Vessels Total Mitosis Events (Mean)*
	Anaphase (Mean)*	Total Mitosis Events (Mean)*	Anaphase (Mean)*	Total Mitosis Events (Mean)*	
RA p6 (n = 6)	26 (4.33)	98 (16.3)	42 (7)	135 (22.5)	233 (38.83)
RA p7 (n = 7)	20 (2.86)	62 (8.86)	59 (8.43)	181 (25.85)	243 (34.71)
RA p11 (n = 6)	10 (1.67)	31 (5.17)	32 (5.33)	111 (18.5)	142 (23.67)
RA p12 (n = 5)	3 (0.6)	7 (1.4)	3 (0.6)	13 (2.6)	20 (4)
RA p14 (n = 5)	0	0	0	0	0
50/10 OIR VEGFab [†] (n = 9)	21 (2.33)	64 (7.1)	50 (5.56)	181 (20.1)	245 (27.22)
50/10 OIR IgG [†] (n = 6)	13 (2.17)	50 (8.83)	39 (6.5)	128 (21.3)	178c (29.67)

* Number of mitotic events/number of retinas.

[†] 50-ng dose.